

AN INTERACTION REGION NEAR THE TOP OF THE IONOSPHERE OBSERVED AT MARS AND VENUS

Authors:

R. A. Frahm, J. D. Winningham, J. R. Sharber, *Southwest Research Institute, San Antonio, TX 78228, USA*, F. Duru, D. A. Gurnett, *University of Iowa, Iowa City, IA 52242, USA*, R. Lundin, *Swedish Institute of Space Physics, Box 812, S98 128 Kiruna, Sweden*, A. J. Coates, S. M. E. Tsang, *Mullard Space Science Laboratory, University College London, Holmbury St. Mary, Dorking, Surrey RH5 6NT, UK*, M. Delva, T. L. Zhang, *Space Research Institute, Austrian Academy of Science, 8042 Graz, Austria*

Abstract

The European Space Agency (ESA) currently operates spacecraft at both Mars (Mars Express - MEx) and at Venus (Venus Express - VEx). Both MEx and VEx contain the Analyzer of Space Plasmas and Energetic Atoms (ASPERA) experiment which measures the electron spectrum with the Electron Spectrometer (ELS) and the ion spectrum with the Ion Mass Analyzer (IMA). The MEx spacecraft also contains the Mars Advanced Radar for Subsurface and Ionospheric Sounding (MARSIS) which can derive the thermal electron density and magnetic field magnitude from its ionograms. The VEx spacecraft also contains a magnetometer (MAG) experiment. At the top of the ionosphere of Mars is a region where there is mixing between plasma from the ionosphere and plasma from the solar wind. ASPERA-3 data from Mars shows the high-energy electron halo/strahl from the solar wind penetrating through the bow shock and magnetosheath into the dayside ionosphere. At the same time, plasma showing electron peaks generated by the ionization of carbon dioxide and atomic oxygen from solar He 30.4 nm penetrates into the magnetosheath. This overlap region is located where the thermal electron density derived by MARSIS decreases and ion plasma begins to accelerate from thermal velocities. This region is also observed at Venus. All three experiments show turbulence near and through the ionosphere/solar wind interaction region.

1. Introduction

The solar wind electron distribution comprises three plasma populations which can be distinguished by particle energy and angular characteristics. These three regions are known as the core, halo, and strahl. The solar wind core is the thermal distribution, typically less than 50 eV. The halo of the solar wind consists of energies greater than the core, is hotter than the core, and has an isotropic angular distribution. In addition to the halo, the strahl component exists in the same energy range as the halo, but its angular distribution is peaked along the solar wind flow direction.

When the solar wind impinges on Mars/Venus, Mars/Venus resists by forming a bow shock and induced magnetic cavity to deflect the solar wind around the planet. The bulk of the flow of the **shocked** solar wind around the planet occurs in the magnetosheath, between the bow shock and ionosphere of the planet; however, a small portion of the **unshocked** solar wind makes contact with and interacts with the ionosphere of the planet.

Solar EUV causes ionization and excitation of a planetary atmosphere, generating an ionosphere. In particular, the 30.4 nm photon ionizes both carbon dioxide (CO_2) and atomic oxygen (O) [Mantas and Hanson, 1979] leading to distinct peaks in the electron spectrum. The photoionized electrons resulting from the interaction with CO_2 and O in the ionospheres of Mars [Lundin et al., 2004] and Venus [Coates et al., 2008] are routinely observed by instruments on board the Mars Express (MEx) and Venus Express (VEx) spacecraft. They can be used as a tracer of the trajectory of dayside ionospheric plasma [Frahm et al., 2006].

At the top of the ionosphere, there exists a region where low-intensity, **unshocked** solar wind plasma mixes with ionospheric plasma, forming a region of transition between plasma which is solar wind dominated and that which is primarily ionospheric. At higher energies (above about 50 eV) the solar wind halo/strahl is observed, and at lower energies (below about 50 eV), ionospheric plasma is observed. The data from Mars and Venus show that within the transition region, both ionospheric and solar wind plasma are observed in varying proportions.

2. Instruments

Data used in this paper from the MEx spacecraft were (1) Analyzer of Space Plasmas and Energetic Atoms (ASPERA-3) [Barabash et al., 2006] (only the Electron Spectrometer-ELS and the Ion Mass Analyzer-IMA) and (2) the Mars Advanced Radar for Subsurface and Ionosphere Sounding [Picardi et al., 2004]. Data analyzed from the VEx spacecraft were (1) Analyzer of Space Plasmas and Energetic Atoms (ASPERA-4) [Barabash et al., 2007] (the Electron Spectrometer-ELS and the Ion Mass Analyzer-IMA) and (2) the Venus Express Magnetometer (MAG) [Zhang et al., 2006].

3. Transition at Mars

Figure 1 shows that the selected example orbit of the MEx spacecraft is near the noon-midnight plane.

Figure 2 shows the electron spectrogram from ELS (top panel) and the ion spectrogram from IMA (bottom panel) to illustrate the context of the spacecraft pass. The intense electron flux between about 0247 UT and about 0254 UT, at less than 20 eV is caused by EUV photoemission from the surface of the spacecraft. The intense ion flux beginning at about 0250 UT is due to UV light contamination in IMA. The core of the solar wind is observed in yellow around 0305 UT with the halo/strahl component of the solar wind at higher energies shown as green. The shocked halo/strahl is seen penetrating into the magnetosheath until about 0222 UT, where the ionosphere is observed. Cold ion fluxes near 10 eV are observed in the ionosphere and keV fluxes are observed in the magnetosheath. Peaks in the ionosphere near 24 eV are observed in the electron spectrogram and are due to photoionization of CO_2 and O. The letters at the top of the spectrographs indicate the location of the selected detailed Spectra.

Figure 3, similar to Figure 2, shows the detailed view of the plasma in the interaction region between the ionosphere and the magnetosheath. The thermal electron density is overlaid on the electron plasma data in the top panel; and the total magnetic field is overlaid on the ion plasma data in the bottom panel, both derived from MARSIS data. The total magnetic field shows a nearly constant value (the deep troughs occur when no magnetic field solution is possible) throughout the figure, indicating that no magnetic anomalies are influencing the plasma measurements. The thermal density shows a transition beginning just before the photoelectron peaks show a flux decrease, and low-energy ions diminish in intensity as the altitude on the spacecraft is increasing (about 02:21:45 UT). It should be noted that these ions are upshifted in energy due to the negative spacecraft potential and their disappearance could be related to a drop in spacecraft potential. At this time, the unshifted solar wind halo/strahl is observed (although less intense than in the magnetosheath). This begins a transition region from the observation of pure ionospheric plasma to pure magnetosheath plasma.

As the thermal density continues to decrease, a mixture of plasma is observed showing both the photoelectron plasma with its characteristic peaks at lower energies and the halo/strahl of the solar wind at higher energies. At about 02:24:55 UT, the thermal density reaches a steady value in the magnetosheath, magnetosheath electrons are observed (**shocked** solar wind plasma) and the halo/strahl intensity has increased. This marks the end of the transition from ionosphere plasma to magnetosheath plasma.

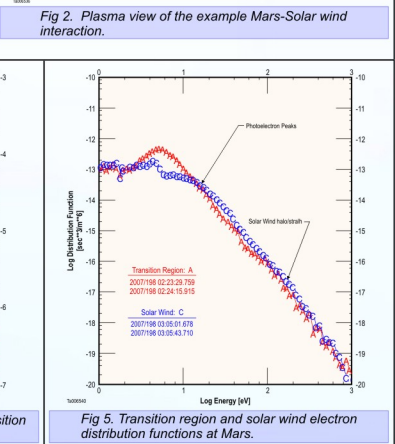
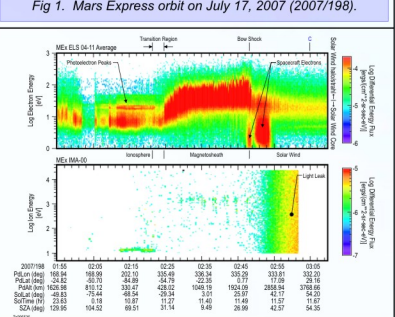
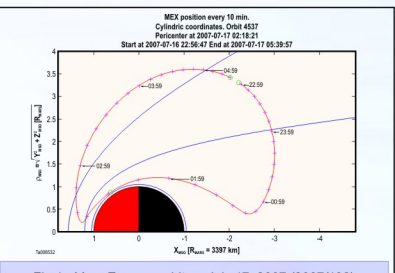
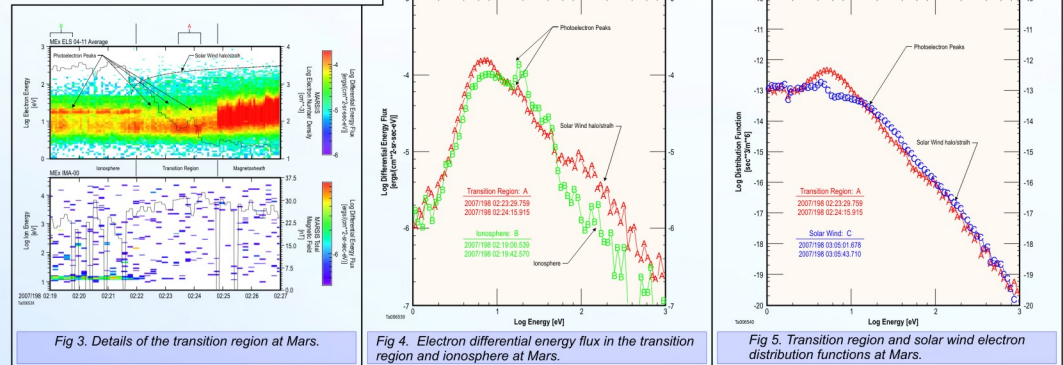


Figure 4 compares the shape of the electron differential energy flux in the transition region with that in the ionosphere. Common features are the dominance of the EUV generated electrons below 50 eV and the photoelectron peaks from CO_2 and O photoionization. At energies greater than 50 eV, the solar wind halo/strahl influence causes a larger flux in the transition region than in the ionosphere.

Figure 5 compares the shape of the electron distribution function in the transition region with that in the solar wind. This figure shows that the shape of the **unshocked** high-energy solar wind halo/strahl is the same as in the transition region. The dominance by photoelectrons in the spectrum is seen below 50 eV in the transition region.

4. Transition at Venus

Figure 6 shows that the selected example orbit of the Venus Express spacecraft is near the noon-midnight plane. The orientation of the VEx at Venus is similar to the orientation MEx at Mars.

Figure 7 shows the electron spectrogram from ELS sectors 04 through 11 to illustrate the context of the spacecraft pass and the differences in the ELS sectors. The intense electron fluxes at less than 30 eV in the magnetosheath are due to positive spacecraft potential (before about 0815 UT). In general, the Venus Express spacecraft charges positively in the solar wind and magnetosheath, and negatively in the ionosphere. The solar wind core is observed at the beginning of the data in yellow and the halo/strahl is observed at higher energies in green to blue. The **shocked** and **unshocked** solar wind halo/strahl is observed to penetrate down to the ionosphere until about 08:17:30 UT.

Figure 8 shows the electron plasma data from ELS sector 4 in each panel with magnetic field component measurements overlaid. Variations in the magnetic field components are observed to be more dynamic inside the bow shock and inside the influence of the planet than in the solar wind. This is most obvious at the bow shock; however, not as strong in the transition region.

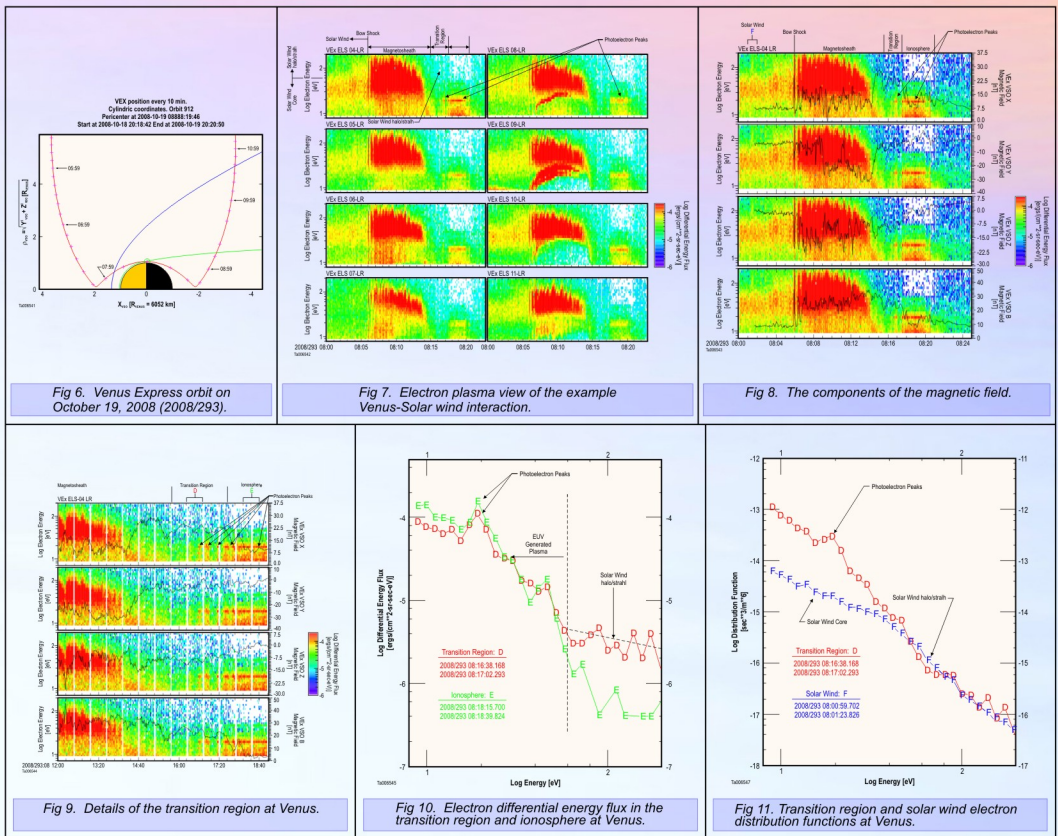


Figure 9 shows a more detailed view of the transition region, the region between magnetosheath plasma and ionosphere plasma, in the same format as Figure 8. Intense and more energetic magnetosheath electron plasma is observed until about 08:14:10 UT, but **unshocked** solar wind electron plasma is observed until about 08:15:45 UT. **Unshocked** solar wind halo/strahl plasma is observed penetrating into the ionosphere until about 08:17:30 UT. Photoelectrons are observed in the region where the **unshocked** solar wind halo/strahl is observed (notice the characteristic O and CO_2 photoelectron peaks at about 08:16:20 UT). Spectra with photoelectrons are observed in the ionosphere.

For this case, both the magnetometer and the electron spectrum are sampled every second. Wave motion is observed in the magnetic field components. Wave motion alone may not cause a strong influence on the flux of photoelectron peaked plasma in the transition region. In the transition region, the magnetic field shows a wave period of roughly 45 sec. Field deviations maximize toward positive X_VSO and negative Z_VSO synchronously; it is not obvious that there are strong deviations in the Y_VSO component. The more intense flux exhibited by the photoelectron peaked plasma occurs when oscillations in the magnetic field components are at a 90 deg phase. However, the flux intensity exhibited by various ELS sectors (see Fig. 7) may be an indication that flux intensity is ordered by the pitch angle. Additional study is needed to uncover the role that the magnetic field variation plays in the photoelectron peak flux in the transition region.

As was done in the Mars data, the transition region spectrum is compared to the ionosphere (Figure 10). The transition region spectrum shows similar photoelectron peaks: a region created by the solar EUV as in the ionosphere and a higher flux at energies greater than 50 eV caused by the penetrating **unshocked** solar wind halo/strahl. An additional comparison of the transition region spectrum with that of the **unshocked** wind in Figure 11 which shows that the shape is similar at energies greater than 50 eV. One notes however, that the magnitude in the transition region is much less than the magnitude in the solar wind.

Spacecraft charging can influence the shape and magnitude of electron distributions. To show its influence and examine the dawn-dusk effect, we show a case for December 16, 2008 (2008/351). The orbit of the VEx spacecraft is shown in figure 12.

The overall context of the plasma is shown in Figure 13, where the electron plasma is shown in the top panel, ion plasma in the center panel, and electron plasma adjusted for the spacecraft potential in the lower panel. The solar wind halo/strahl is not as visible as in the previous cases due to the characteristics of the solar wind; however, ion intensities in the sheath are much stronger. The transition regions is observed on both the dawn and dusk sides of the planet.

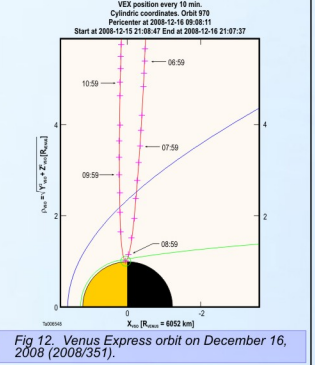
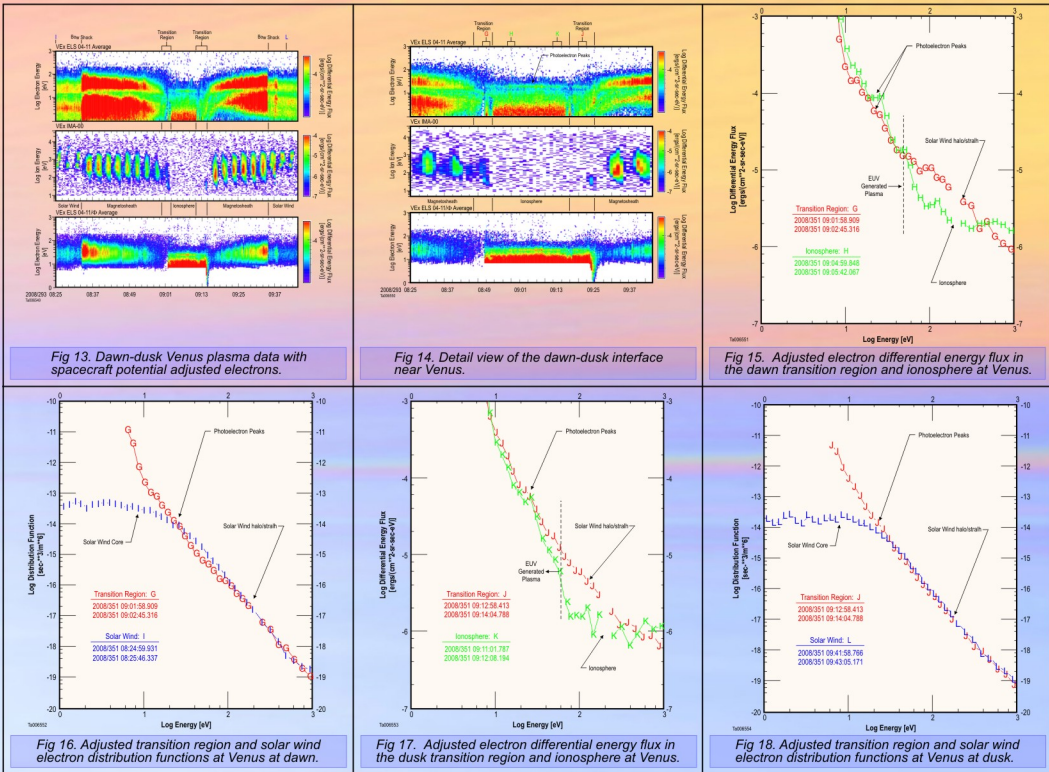


Figure 14 shows more detail of the dawn and dusk transition region. In the unadjusted electron spectrogram, low-energy plasma in the magnetosheath is observed increasing quickly to magnetosheath energies, before about 09:01:30 UT on the dawn side and after about 0912 UT on the dusk side. However, the adjusted data suggest that the low-energy is an effect of the spacecraft potential and only the high-energy halo/strahl is observed.

In addition, ions are observed in the transition region. These observations indicate that higher energy ions are observed in the transition region and lower energy ions are observed in the ionosphere. These observations also indicate that the ion energy is less in the transition region than in the magnetosheath.

This is confirmed by examining dawn spectra, shown in Figure 15 and Figure 16, in the transition region. The adjusted plasma from the ionosphere (Figure 15) shows that the photoionization peaks are present in both the ionosphere and transition region, and the greater than 50 eV plasma shows a different slope in the ionosphere than in the transition region. However, the slope of the electrons greater than 50 eV matches the halo/strahl component of the **unshocked** solar wind (Figure 16), indicating that solar wind is mixing in the transition region.

This is also confirmed by examining dusk spectra, shown in Figure 17 and Figure 18, in the transition region. The adjusted plasma from the ionosphere (Figure 17) shows that the photoionization peaks are present in both the ionosphere and transition region, and the greater than 50 eV plasma shows a different slope in the ionosphere than in the transition region. However, the slope of the electrons greater than 50 eV matches the **unshocked** halo/strahl component of the solar wind (Figure 18), indicating that **unshocked** solar wind is mixing in the transition region.



5. Conclusion

There exists a region between the lower altitude magnetosheath and upper altitude ionosphere which acts as a transition between two different plasmas. In this transition region, both low-energy plasma from the ionosphere and high-energy **unshocked** plasma from the solar wind can exist simultaneously at both Mars and Venus. This transition region is caused by the direct impact of the **unshocked** solar wind on the atmospheres of Mars and Venus. The nearest analog to similar regions at the Earth is its cusps. However, a search for upflowing photoelectrons in the cusps has determined that such observations are extremely rare. A likely explanation is the suppression of the photoelectron population by an ambipolar electric field known to be present in the Earth's polar upper atmosphere. The Earth cusp is not an exact analog since the **unshocked** solar wind is observed at the top of the ionosphere of Mars and Venus, whereas in the Earth cusp, solar wind plasma has been **shocked**. The transition region may be unique to both Mars and Venus and most likely indicates a magnetic connection far down the tail at a location where the **shock** is non-existent (the solar wind electrons do not indicate transmittal through an electric **shock** potential).

6. Acknowledgements

We wish to acknowledge support through the National Aeronautics and Space Administration (NASA) contract NASW-00003 in the United States at SwRI and support by NASA through the Jet Propulsion Laboratory (JPL) contract 1224107 with the University of Iowa, the Particle Physics and Astronomy Research Council (PPARC) in the United Kingdom, and the Swedish National Space Board for their support of the main PI-institute. In addition, we would like to thank C. A. Gonzalez, S. J. Jeffers, J. Mukherjee, and M. Muller at SwRI for their computational assistance.

7. References

- Barabash et al., "The Analyzer of Space Plasmas and Energetic Atoms (ASPERA-3) for the Mars Express mission," *Space Science Reviews*, 126, 113-164, 2006.
- Barabash et al., "The Analyzer of Space Plasmas and Energetic Atoms (ASPERA-4) for the Venus Express mission," *Planetary and Space Science*, 55, 1772-1792, 2007.
- Coates et al., "Ionospheric photoelectrons at Venus: Initial observations by ASPERA-4 ELS," *Planetary and Space Science*, 56, 802-806, 2008.
- Frahm et al., "Locations of Atmospheric Photoelectron Energy Peaks within the Mars Environment," *Space Science Reviews*, 126, 389-402, 2006.
- Lundin et al., "Solar wind-induced atmospheric erosion on Mars: First results from ASPERA-3 on Mars Express," *Science*, 305, 1933-1936, 2004.
- Mantas and Hanson, "Photoelectron fluxes in the Martian ionosphere," *J. Geophys. Res.*, 84, 369-385, 1979.
- Picardi et al., "MARSIS: Mars Advanced Radar for Subsurface and Ionosphere Sounding," in *Mars Express: A European Mission to the Red Planet*, A. Wilson editor, ESA Publication SP-1240, Noordwijk, Netherlands, 51-69, 2004.
- Zhang et al., "Magnetic field investigation for the Venus plasma environment: Expected new results from Venus Express," *Planetary and Space Science*, 54, 1336-1343, 2006.

